Nanostructured black silicon and the optical reflectance of graded-density surfaces

Howard M. Branz, Vernon E. Yost, Scott Ward, Kim M. Jones, Bobby To, and Paul Stradins

Citation: Appl. Phys. Lett. **94**, 231121 (2009); doi: 10.1063/1.3152244
View online: https://doi.org/10.1063/1.3152244
View Table of Contents: http://aip.scitation.org/toc/apl/94/23
Published by the American Institute of Physics

Articles you may be interested in

Efficient black silicon solar cell with a density-graded nanoporous surface: Optical properties, performance limitations, and design rules
Applied Physics Letters **95**, 123501 (2009); 10.1063/1.3231438

Black nonreflecting silicon surfaces for solar cells
Applied Physics Letters **88**, 203107 (2006); 10.1063/1.2204573

Wide-band “black silicon” based on porous silicon
Applied Physics Letters **88**, 171907 (2006); 10.1063/1.2199593

Multi-scale surface texture to improve blue response of nanoporous black silicon solar cells
Applied Physics Letters **99**, 103501 (2011); 10.1063/1.3636105

Near-unity below-band-gap absorption by microstructured silicon
Applied Physics Letters **78**, 1850 (2001); 10.1063/1.1358846

The structural and optical properties of black silicon by inductively coupled plasma reactive ion etching
Journal of Applied Physics **116**, 173503 (2014); 10.1063/1.4900996

PHYSICS TODAY
WHITEPAPERS

MANAGER'S GUIDE

Accelerate R&D with
Multiphysics Simulation

READ NOW

PRESENTED BY

Nanostructured black silicon and the optical reflectance of graded-density surfaces

Howard M. Branz,[a] Vernon E. Yost, Scott Ward, Kim M. Jones, Bobby To, and Paul Stradins
National Renewable Energy Laboratory, 1617 Cole Boulevard, Golden, Colorado 80401, USA

(Received 13 April 2009; accepted 19 May 2009; published online 11 June 2009)

We fabricate and measure graded-index "black silicon" surfaces and find the underlying scaling law governing reflectance. Wet etching (100) silicon in $HAuCl_4$, HF, and H_2O_2 produces Au nanoparticles that catalyze formation of a network of [100]-oriented nanopores. This network grades the near-surface optical constants and reduces reflectance to below 2% at wavelengths from 300 to 1000 nm. As the density-grade depth increases, reflectance decreases exponentially with a characteristic grade depth of about 1/8 the vacuum wavelength or half the wavelength in Si. Observation of Au nanoparticles at the ends of cylindrical nanopores confirms local catalytic action of moving Au nanoparticles. © *2009 American Institute of Physics*. [DOI: 10.1063/1.3152244]

Photovoltaic cells and photon detectors incorporate antireflective single or multilayer thin films deposited on the semiconductor surface. However, subwavelength surface texture on silicon is known to produce "black silicon" with a broadband antireflection at a far wider acceptance angle than single or multilayer antireflection films.[1–5] This nanometer-scale texture also increases the Si surface area for other applications.[6–8] Black silicon texture has been produced by techniques including laser-chemical,[1] electrochemical,[2] and reactive-ion etching.[9] Some techniques produce regular nanoscale "moth-eye" texture[10] but random textures can suppress reflection equally well. Stephens and Cody (SC) (Ref. 11) proposed that an optical-constant gradient eliminates the sharp air-silicon interface which would reflect electromagnetic radiation. Porous features must be much smaller than the wavelength, λ, of the incident light. Nanoscale features are therefore needed to suppress reflection down to 300 nm for photovoltaic devices.

Because black Si needs nanoscale features, nanotechnology fabrication methods should be beneficial. For widespread application to photovoltaic technology, these techniques should also be inexpensive. In this letter, we describe two distinct single-step etch techniques that use gold nanoparticles (or a nanoparticle-producing compound) mixed with HF and H_2O_2 to produce black silicon. Previous workers have used evaporated nanoscale Au islands,[3] plated gold,[4] or deposited silver[5] nanoparticles to produce textured silicon but these techniques would likely be costlier than our single-step etch processes.

SC (Ref. 11) provided computer solutions for reflection from several graded-density surface texture models of silicon and of glass. They scaled the incident λ by the grade depth and found that the *computed* reflectance from several density graded layers were functions of the depth-scaled λ. However, SC (Ref. 11) did not investigate the universality of this scaling. While intuitively appealing, the scaling of λ by depth is neither proven generally nor tested experimentally. For this letter, we *measure* the spectral dependence of reflectance, $R(\lambda)$, at intervals during the black etch and determine the grade depth, d, of the nanoporous surfaces by scanning electron microscopy (SEM). We find that R decreases exponentially with d/λ according to a robust scaling law.

Both black Si etchants are made by mixing $HF:H_2O_2:H_2O$ in the ratio of 1:5:2 with an equal volume of an aqueous gold-containing solution. The resulting HF and H_2O_2 dilutions in water are the same as previously used to black-etch Si.[3] Without added gold, we observe no R change. For black Si, we mix 5 nm colloidal gold particles in water (5×10^{13}/ml, Ted Pella) into an equal volume of the 1:5:2 solution in a beaker containing the silicon wafer and stir ultrasonically. The minimum reflectance is reached in about 15 min. As a faster and less expensive alternative, we cover the silicon wafer with 0.4 mM $HAuCl_4$ solution and then add an equal quantity of the 1:5:2 $HF:H_2O_2:H_2O$ solution. Minimum reflectance is reached in less than 2 min. The formation of gold nanoparticles due to reduction of $HAuCl_4$ by the hydrogen peroxide[12] is indicated by a rapid purple coloration of the solution.[13] We have confirmed nanoparticle formation by placing a droplet of the used etch solution onto a transmission electron microscopy (TEM) grid and imaging the 20–100 nm diameter particles. Surface gold contamination from either etch can be removed[3] in I_2/KI or aqua regia. We are able to black etch Si of various orientations, dopant types, and resistivities but results reported here are all on polished (100) surfaces of p-type 1–2 Ω cm B-doped Czochralski Si wafers. Our chemicals are all complementary metal-oxide-semiconductor reagent grade (Mallinckrodt Baker) and are diluted with 10 MΩ cm de-ionized water.

After black etches of different duration, we measure total hemispheric reflectance spectra in air on a Varian Cary 6000i spectrophotometer with an integrating sphere. Etch depths are determined by digitally analyzing SEM images taken of cross sections of the etched wafers by computerized correlation analysis of pixel intensities along lines parallel to the etched surface. Higher electron emission from near-surface regions may result in systematic error up to about 20 nm in the thickness of the density-graded layers.

Figure 1 shows typical SEM images of the (011) fracture plane after each etch. Nanopores are very dense near the surface and often cluster into wider pores. Progressively fewer long nanopores extend more deeply, resulting in

[a]Electronic mail: howard.branz@nrel.gov.

 © 2009 American Institute of Physics

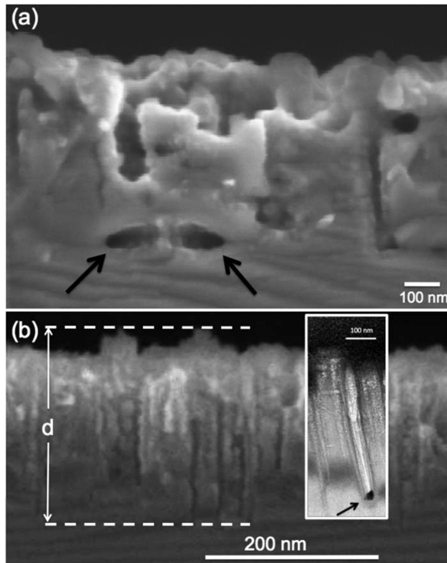

FIG. 1. Cross-sectional SEM images of the (100) Si surface etched in (a) colloidal Au solution for 900 s, with arrows indicating nanopores entering the (011) cleavage plane. (b) $HAuCl_4$ solution for 80 s, with dashed lines indicating extrema of the density-grade depth found by computerized pixel correlation analysis. Inset to (b) is dark-field TEM (100-nm scalebar) of a nanopore and Au particle (indicated by arrow) produced by $HAuCl_4$ solution etching.

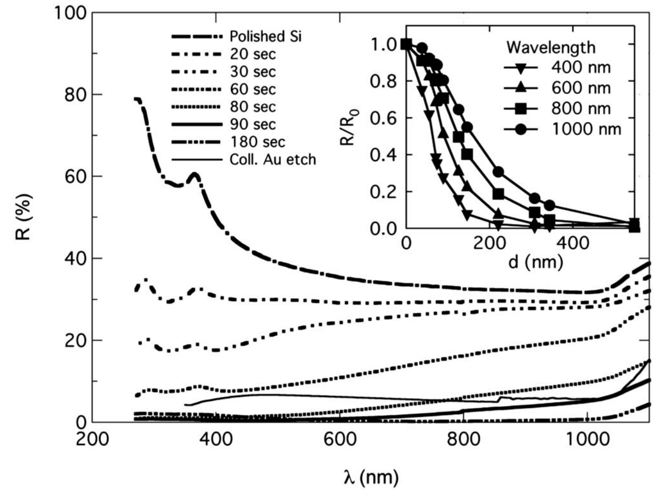

FIG. 2. Reflectance spectra taken after etching in $HAuCl_4$ black-etch solution for 80 s [SEM of Fig. 1(b)] and other times, as indicated; additional spectrum taken after 900 s etch in colloidal Au solution [SEM of Fig. 1(a)]. Inset shows R at indicated wavelengths, normalized to the polished wafer ($d=0$), vs density-grade depth, d.

density-graded surface layers; quantitative analysis of a TEM cross section of a $HAuCl_4$-etched sample reveals that the density increases roughly linearly with depth. Figure 1(a) shows that etching 15 min with 5 nm colloidal Au creates high-aspect-ratio nanopores with diameters of 20–50 nm, as deep as 500 nm. The nanopores follow [100] vectors from the surface into the wafer, with infrequent perpendicular turns to [010] and [001] directions (arrows). Figure 1(b) shows that 80 s etching in the $HAuCl_4$ solution produces a similar morphology, with narrower nanopores, 5–20 nm in diameter and up to 200 nm long.

The dark field TEM (Tecnai TF20-UT) image inset in Fig. 1(b) shows a Au nanoparticle left at the end of a nanopore after etching for 100 s in the $HAuCl_4$ mixture. Energy dispersive x-ray spectroscopy in the TEM of several such nanoparticles confirms they are Au. We conclude that the nanopore formation mechanism is Au catalyzed[14] in both our etchant mixtures; catalytic decomposition of H_2O_2 at the Au nanoparticle surface causes rapid local oxidation of the silicon, which is followed by HF etch of the SiO_2 (Ref. 15) to produce nanopores a few times larger than the nanoparticle size. Because the (100) surface is far more vulnerable to oxidation than is the (111) surface,[16] the nanoparticle moves into the silicon mainly along [100], [010], and [001] directions, driven by some combination of Brownian motion, ultrasonic agitation, and bubbles of gaseous reaction products.

Figure 2 compares the total reflectance spectra of a polished (100) Si wafer to identical wafers etched in the 5 nm colloidal Au solution for 900 s and in the $HAuCl_4$ solution for 20–180 s. Black Si R rises at $\lambda > 1000$ nm where the wafer becomes optically transparent, due to light reflected from the wafer back surface and sample holder. Figure 2 shows that R from the sample etched with colloidal Au is below about 8% from 300 to 1000 nm; other such samples had R below 5%. The $HAuCl_4$ black etch reduces (100) silicon surface reflectance to below 2% and other surface orientations to below 10%.

We convert the $HAuCl_4$ black-etch time series $R(\lambda,t)$ to the depth dependence $R(d)$ at several values of λ to reveal the optical physics of graded density black-Si layers. The inset of Fig. 3 shows that reflections of the shortest λ light are suppressed after the shallowest etches, with progressively longer λ suppressed by deeper density grades. A slight recovery of the R below 400 nm, beginning after about 90 s, is likely due to development of larger-scale surface features that scatter incident short-wavelength light.

In Fig. 3, we plot on semilog axes the reflectances (normalized to the polished wafer) after $HAuCl_4$-solution etching for times from 10 to 90 s. The abscissa of each curve is now d/λ; we plot reflectivity versus the inverse of λ scaled by the grade depth of each individual sample. Reflectance curves taken after the shortest etch times appear at the upper left corner (small d, high R). Ignoring the data below 400 nm where the scattering effects apparently become important (blue curves in Fig. 3), reveals a robust scaling law for R

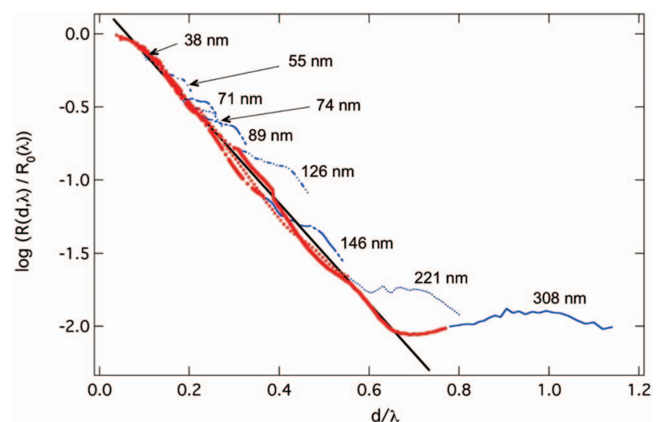

FIG. 3. (Color) Reflectance of Si after $HAuCl_4$ solution etches lasting 10–90 s (10 s intervals). Each curve is labeled by its density-grade depth. R is normalized to polished wafer ($d=0$) and plotted vs d scaled by λ. Due to light scattering, blue tails of each R curve ($\lambda < 400$ nm) are not included in the exponential fit (solid line) to the rest of the data.

between 400 and 1000 nm (red curves). The reflectance of the etched wafer falls exponentially with increasing d/λ from the polished Si values of $R_0(\lambda)$,

$$R(d,\lambda) = R_0(\lambda)e^{-C\cdot(d/\lambda)}. \quad (1)$$

A best fit to Eq. (1) of the data on all curves between 400 and 1000 nm yields $C \sim 7.8$, and this fit line is plotted in Fig. 3. As the density-grade depth increases with etch time, R decreases exponentially with a characteristic depth of about $\lambda/8$.

The collapse of all $R(\lambda)$ curves in Fig. 2 onto a universal $R(d/\lambda)$ curve in Fig. 3 demonstrates that the ratio of the thickness grade depth to λ is the critical dimensionless parameter controlling the suppression of surface reflectance. The excellent fit of the decay curves means that Eq. (1) provides a robust scaling law valid when scattering effects are unimportant. Reflection at optical density steps depends upon an interface sharp compared with λ. For reflection at the shortest wavelengths, only a very abrupt density grade is "sharp." A nanopore or grade depth of $\sim$250 nm is required to reduce R/R_0 to below 5% out to 1000 nm. This estimate sets the required grade depth nearly equal to the wavelength of the light in the Si itself (index 3.5–5.5), a rule-of-thumb applicable to producing black surfaces in other materials by surface density grading.

In conclusion, we demonstrate two nanoparticle-based etchants for Si which form a graded-density black silicon surface layer of a network of nanopores. Surface reflectance can be as low as 2% from 300 to 1000 nm, with no antireflection coating. As the density-graded layer grows deeper, the reflection of progressively longer wavelength light is suppressed. Reflectance spectra taken from a grade-depth series reveal a universal exponential decay of the reflectance when plotted against d/λ. The characteristic decay depth of the grade is about $\lambda/8$.

The authors are grateful to many NREL colleagues. D. Ginley provided helpful discussions of the chemistry and A. Duda, H.-C. Yuan, and M. Page made valuable suggestions. This work was supported by the U.S. Department of Energy under Contract No. DE-AC36-08GO28308.

[1] C. Wu, C. H. Crouch, L. Zhao, J. E. Carey, R. Younkin, J. A. Levinson, E. Mazur, R. M. Farrell, P. Gothoskar, and A. Karger, Appl. Phys. Lett. **78**, 1850 (2001).
[2] L. L. Ma, Y. C. Zhou, N. Jiang, X. Lu, J. Shao, W. Lu, J. Ge, X. M. Ding, and X. Y. Hou, Appl. Phys. Lett. **88**, 171907 (2006).
[3] S. Koynov, M. S. Brandt, and M. Stutzmann, Appl. Phys. Lett. **88**, 203107 (2006).
[4] K. Nishioka, S. Horita, K. Ohdaira, and H. Matsumura, Sol. Energy Mater. Sol. Cells **92**, 919 (2008).
[5] K. Tsujino, M. Matsumura, and Y. Nishimoto, Sol. Energy Mater. Sol. Cells **90**, 100 (2006).
[6] M. Rournanie, C. Delattre, F. Mittler, G. Marchand, V. Meille, C. de Bellefon, C. Pijolat, G. Tournier, and P. Pouteau, Chem. Eng. J. **135**, S317 (2008).
[7] P. Hoyer, M. Theuer, R. Beigang, and E. B. Kley, Appl. Phys. Lett. **93**, 091106 (2008).
[8] M. Stubenrauch, M. Fischer, C. Kremin, M. Hoffmann, and J. Muller, Micro & Nano Lett. **2**, 6 (2007).
[9] T. P. Chow, P. A. Maciel, and G. M. Fanelli, J. Electrochem. Soc. **134**, 1281 (1987).
[10] S. J. Wilson and M. C. Hutley, Opt. Acta **29**, 993 (1982).
[11] R. B. Stephens and G. D. Cody, Thin Solid Films **45**, 19 (1977).
[12] T. K. Sarma, D. Chowdhury, A. Paul, and A. Chattopadhyay, Chem. Commun. (Cambridge) **2002**, 1048.
[13] J. P. Wilcoxon, R. L. Williamson, and R. Baughman, J. Chem. Phys. **98**, 9933 (1993).
[14] X. Li and P. W. Bohn, Appl. Phys. Lett. **77**, 2572 (2000).
[15] K. Tsujino and M. Matsumura, Adv. Mater. (Weinheim, Ger.) **17**, 1045 (2005).
[16] D. Graf, S. Bauermayer, and A. Schnegg, J. Appl. Phys. **74**, 1679 (1993).